

Bayesian Effect Selection in Additive Models with an Application to Time-to-Event Data

Paul Bach and Nadja Klein

Chair of Uncertainty Quantification and Statistical Learning
Research Center Trustworthy Data Science and Security (UA Ruhr) and
Department of Statistics (Technische Universität Dortmund)
Joseph-von-Fraunhofer Straße 25, 44227 Dortmund

January 2, 2024

Abstract

Accurately selecting and estimating smooth functional effects in additive models with potentially many functions is a challenging task. We introduce a novel Demmler-Reinsch basis expansion to model the functional effects that allows us to orthogonally decompose an effect into its linear and nonlinear parts. We show that our representation allows to consistently estimate both parts as opposed to commonly employed mixed model representations. Equipping the reparameterized regression coefficients with normal beta prime spike and slab priors allows us to determine whether a continuous covariate has a linear, a nonlinear or no effect at all. We provide new theoretical results for the prior and a compelling explanation for its superior Markov chain Monte Carlo mixing performance compared to the spike-and-slab group lasso. We establish an efficient posterior estimation scheme and illustrate our approach along effect selection on the hazard rate of a time-to-event response in the geoadditive Cox regression model in simulations and data on survival with leukemia.

Keywords: Demmler-Reinsch; effect decomposition; group selection; mixed model representation; partially linear; penalized splines.

1 Introduction

Suppose we have data $\mathcal{D} = \{(y_i, \mathbf{x}_i), i = 1, \dots, n\}$, where the y_i are univariate response values and the $\mathbf{x}_i \in \mathbb{R}^p$ are vectors of covariates. A common model assumption is the generalized additive model (GAM; [Hastie and Tibshirani, 1986, 1990](#)), where $Y | \mathbf{X} = (X_1, \dots, X_p)^T$ follows an exponential family distribution and the conditional mean is expressed as

$$g(\mathbb{E}[Y | \mathbf{X}]) = \beta_0^* + \sum_{j=1}^p f_j^*(X_j), \quad (1)$$

where $g(\cdot)$ is a suitable link function and $\mathbb{E}[f_j^*(X_j)] = 0$, $j = 1, \dots, p$, to ensure identifiability. The selection and estimation of functional effects in the GAM (1) is a highly relevant problem with applications in many disciplines such as biostatistics, ecology or economics ([Wood, 2017](#); [Fahrmeir et al., 2021](#)). In this framework, the additive components f_j^* are often modeled using basis expansions such as polynomials, splines or trigonometric functions. By doing so, function selection in the GAM (1) can be cast into a group selection problem in a generalized linear model framework with many available options such as the group lasso ([Yuan and Lin, 2006](#)), the sparse additive model ([Ravikumar et al., 2009](#)), the Bayesian group lasso ([Kyung et al., 2010](#)) or the nonparametric spike-and-slab lasso ([Bai et al., 2022](#)).

These methods, however, follow an “all-in-all-out” approach for function selection ([Guo et al., 2022](#)). That is, they do not allow to decide whether a nonlinear effect is actually necessary to model a selected covariate or whether a linear effect is already sufficient. This is suboptimal because a linear effect is easier to interpret and reduces model complexity, thereby helping to avoid overly wiggly estimates when modeling a truly linear effect in a nonlinear fashion ([Lou et al., 2016](#); [Guo et al., 2022](#); [Russell and Rubio, 2023](#)). In recent years, several methods addressing this shortcoming have been proposed. Penalized likelihood approaches include the linear and nonlinear discoverer ([Zhang et al., 2011](#)), generalized additive model selection ([Chouldechova and Hastie, 2015](#)) and the sparse partially linear additive model ([Lou et al., 2016](#)). Another option is model-based boosting ([Hofner et al., 2014](#)) and Bayesian approaches include the methods of [Scheipl et al. \(2012\)](#); [Hu et al. \(2015\)](#); [He and Wand \(2023\)](#) as well as non-local priors ([Russell and Rubio, 2023](#)). For estimation, most of these methods decompose an additive component f_j

into a sum of the form

$$f_j = f_{j,lin} + f_{j,nonlin} = \tilde{x}_j \beta_j + \sum_{l=1}^{d_j} \phi_{j,l}(x_j) u_{j,l}, \quad (2)$$

where \tilde{x}_j is a linear function that is standardized empirically and the $\phi_{j,l}$, $l = 1, \dots, d_j$, are some basis functions that are supposed to capture the nonlinear covariate effect. Applying such a decomposition to all f_j , for $j = 1, \dots, p$, the additive predictor reads as follows

$$\eta(\mathbf{x}) = \beta_0 + \sum_{j=1}^p \beta_j \tilde{x}_j + \sum_{j=1}^p \sum_{l=1}^{d_j} \phi_{j,l}(x_j) u_{j,l}. \quad (3)$$

For the vector of predictor evaluations $\boldsymbol{\eta} = (\eta(\mathbf{x}_1), \dots, \eta(\mathbf{x}_n))^T$ we thus obtain in matrix notation

$$\boldsymbol{\eta} = \beta_0 \mathbf{1}_n + \sum_{j=1}^p \beta_j \tilde{\mathbf{x}}_j + \sum_{j=1}^p \mathbf{Z}_j \mathbf{u}_j, \quad (4)$$

where $\mathbf{1}_n = (1, \dots, 1)^T$ is a column vector of n ones, $\tilde{\mathbf{x}}_j = (\tilde{x}_{1j}, \dots, \tilde{x}_{nj})^T$ are the standardized covariate vectors with zero mean and unit variance and $\mathbf{Z}_j = (\phi_{j,l}(x_{ij}))_{i=1, \dots, n, l=1, \dots, d_j} \in \mathbb{R}^{n \times d_j}$ are design matrices of basis function evaluations for $j = 1, \dots, p$. To achieve sparsity, the coefficients β_j and \mathbf{u}_j in (4) are endowed with separate shrinkage penalties or priors.

While the procedure seems to be straightforward at first sight, we argue that there are two important, interrelated questions to which the existing references provide only partially satisfactory answers:

- Q1: Does it suffice that the linear functions $\text{span}\{1, x_j\}$ are not contained in the span of the nonlinear basis functions $\text{span}\{\phi_{j,1}, \dots, \phi_{j,d_j}\}$ or do we need an orthogonal decomposition in (2) such that $\text{span}\{1, x_j\} \perp \text{span}\{\phi_{j,1}, \dots, \phi_{j,d_j}\}$?
- Q2: What exactly are the estimands (Berk, 2008) of $f_{j,lin}$ and $f_{j,nonlin}$ in (2)? Phrased differently, what exactly are the true linear $f_{j,lin}^*$ and nonlinear effect $f_{j,nonlin}^*$ of an additive component f_j^* in model (1)?

Regarding Q1: Some of the references do impose orthogonality in (2), others do not. Scheipl et al. (2012) and Rossell and Rubio (2023), for instance, explicitly enforce empirical orthogonality in (2) arguing that this leads to a better effect separation or gains in power, respectively. Hofner et al. (2014) and Guo et al. (2022), in contrast, use mixed model representations (MMRs) of penalized splines. Guo et al. (2022) use the spectral decomposition of the penalty matrix as

suggested by [Fahrmeir et al. \(2004\)](#), whereas [Hofner et al. \(2014\)](#) use Eiler’s transformation ([Eilers, 1999](#)) based on the P-splines differences matrix ([Eilers and Marx, 1996](#)). In both cases, the resulting spline basis functions are not orthogonal to the linear functions. [Hu et al. \(2015\)](#) use centered truncated power series functions for the nonlinear basis functions. These functions are not orthogonal either but in general even highly correlated with the linear functions.

Regarding Q2: Remarkably, only [Zhang et al. \(2011\)](#) provide a rigorous definition of the true linear and nonlinear effect of an additive component f_j^* , while such a definition seems to be missing in the other references. However, [Zhang et al. \(2011\)](#) use a reproducing kernel Hilbert framework as in [Wahba \(1990\)](#), which does not easily translate to general basis expansion approaches. We opt for a different strategy based on projections, which appears more natural in this context, and provides elegant answers to both questions above.

More specifically, we define the true linear effect of an additive component f_j^* in (1) as the $\mathcal{L}^2(\mathbb{P}^{X_j})$ -projection onto the linear functions. With this, the true linear effect is defined as the unique linear function that is as close as possible to f_j^* in the sense of the $\mathcal{L}^2(\mathbb{P}^{X_j})$ -norm. The true nonlinear effect is defined as the residual of this projection.

For estimation, we expand the nonlinear effects in Demmler-Reinsch (DR) spline bases. The DR basis originates from the smoothing splines literature ([Demmler and Reinsch, 1975](#)) and is characterized by simultaneous orthogonality with respect to the empirical inner product and the differential semi-inner product associated with the smoothing spline roughness penalty (see [Speckman, 1985](#), Eq. 2.1). For the computationally much more convenient P-splines ([Eilers and Marx, 1996](#); [Lang and Brezger, 2004](#)) with less spline knots than observations, the DR basis is not as popular as the MMRs of [Eilers \(1999\)](#); [Fahrmeir et al. \(2004\)](#). This is presumably because previous constructions of the DR basis in this context were either too restrictive (e.g., [Nychka and Cummins, 1996](#)) or too computationally intensive (e.g., [Scheipl et al., 2012](#)). We suggest a new construction of the DR basis for P-splines, which is less restrictive and more efficient than the previous suggestions.

To perform Bayesian effect selection, we endow the linear coefficients and the DR coefficient vectors with the recently proposed normal beta prime spike and slab (NBPSS) prior of [Klein et al. \(2021\)](#). NBPSS is a continuous group selection prior similar to the popular spike-and-slab group lasso (SSGL) prior of [Bai et al. \(2022\)](#). We compare the two priors in simulations and

observe that NBPSS shows much better Markov chain Monte Carlo (MCMC) mixing for the latent binary selection indicators, especially if the group dimensions are not small. To provide an explanation, we establish new theoretical results for the two priors. In particular, we derive and investigate the implied spike and slab of the Euclidean norm of the group coefficient vectors. We find that the overlap is much bigger for NBPSS, providing a compelling explanation for its superior mixing performance.

Combining the DR bases and NBPSS, we obtain a versatile fully Bayesian approach that allows to perform data-driven effect selection with uncertainty quantification in GAMs and beyond. We illustrate the efficacy of the developed methodology along the geoadditive Cox model (Hennnerfeind et al., 2006) using the leukemia survival data of Henderson et al. (2002). In addition to continuous covariates, the model contains a spatial effect and we also allow for flexible Bayesian estimation of the baseline hazard rate. We conduct simulations comparing our approach with the boosting approach of Hofner et al. (2014) and find that we outperform these authors in terms of both, estimation and selection accuracy.

In summary, the main contributions of this paper are as follows.

- We provide a rigorous definition of a GAM with effect decomposition based on projections and highlight the importance of orthogonality to achieve consistent effect estimation.
- We introduce a new construction of the DR basis for P-splines. This construction is less restrictive and more efficient than previous suggestions.
- We establish new theoretical results for the NBPSS prior. In particular, we derive the implied spike and slab of the Euclidean norm, which provides a compelling explanation for its superior MCMC mixing compared to the SSGL prior for large dimensional groups.
- We illustrate the developed methodology in the geoadditive Cox model. In addition to linear and nonlinear effects of continuous covariates, the model contains several dummy variables and a spatial effect, all of which are subject to data-driven effect selection.

The rest of this paper is structured as follows. In Section 2 we formally introduce the GAM with effect decomposition based on projections and detail our new construction of the DR basis for P-splines. Moreover, we demonstrate that the DR basis is well-suited for the GAM with

effect decomposition, whereas the MMR yields heavily biased effect estimates. In Section 3 we review the NBPSS prior for Bayesian effect selection and establish new theoretical results for the prior in Section 4. Section 5 illustrates the developed methodology in the context of survival data, while Section 6 concludes with a discussion. The supplementary material contains several appendices with further technical details, simulation results and proofs of our theoretical results.

2 GAM with Effect Decomposition Based on Projections

The cornerstone of our method is to decompose a true additive component f_j^* in (1) into the sum $f_j^* = f_{j,lin}^* + f_{j,nonlin}^*$, where $f_{j,lin}^*$ is the $\mathcal{L}^2(\mathbb{P}^{X_j})$ -projection of f_j^* onto the linear functions $span\{1, x_j\}$ and $f_{j,nonlin}^*$ is the corresponding residual. This is made precise in Definition 1.

Definition 1 (Effect decomposition). Let $X_j \in \mathcal{X}_j \subseteq \mathbb{R}$ with distribution \mathbb{P}^{X_j} such that $\mathbb{E}[X_j^2] < \infty$ and $\text{Var}(X_j) > 0$. Then, for a square-integrable additive component $f_j^* : \mathcal{X}_j \rightarrow \mathbb{R}$ we define

$$f_{j,lin}^* := \underset{g_j \in span\{1, x_j\}}{\operatorname{argmin}} \mathbb{E}[(f_j^*(X_j) - g_j(X_j))^2] \quad \text{and} \quad f_{j,nonlin}^* := f_j^* - f_{j,lin}^*. \quad (5)$$

We refer to $f_{j,lin}^*$ as true linear effect and to $f_{j,nonlin}^*$ as true nonlinear effect. Since $f_j^* = f_{j,lin}^* + f_{j,nonlin}^*$, we also refer to f_j^* as true overall effect.

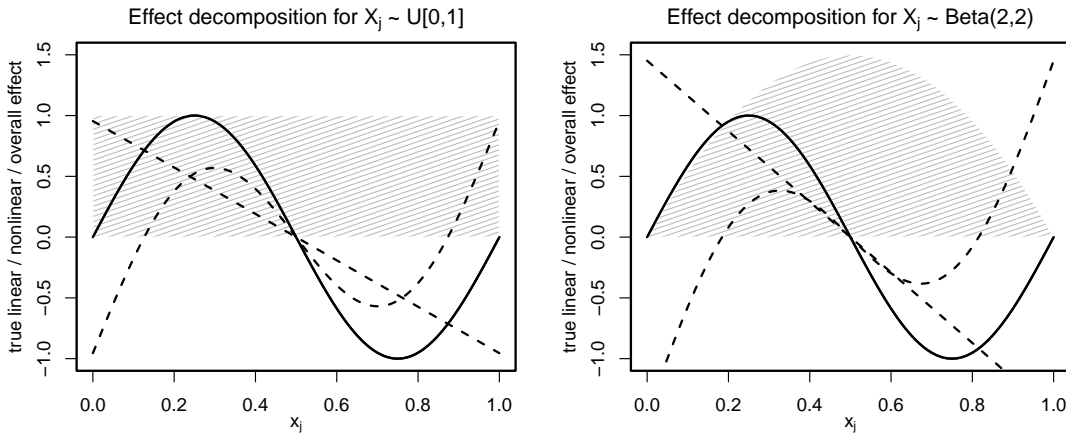


Figure 1: Effect decomposition based on $\mathcal{L}^2(\mathbb{P}^{X_j})$ -projections. Shown are the true additive component $f_j^* = \sin(2\pi x_j)$ (solid) together with its true linear and nonlinear effects (dashed) under a uniform design $X_j \sim U[0, 1]$ (left) and a beta design $X_j \sim Beta(2, 2)$ (right). The shaded gray area depicts the corresponding design density.

For illustration, consider the function $f_j^* = \sin(2\pi x_j)$. Under a uniform design $X_j \sim U[0, 1]$, we obtain the decomposition

$$f_j^* = f_{j,lin}^* + f_{j,nonlin}^* = \{-6/\pi(x_j - 1/2)\} + \{\sin(2\pi x_j) + 6/\pi(x_j - 1/2)\}.$$

Under a beta design $X_j \sim Beta(2, 2)$, we obtain in contrast

$$f_j^* = f_{j,lin}^* + f_{j,nonlin}^* = \{-90/\pi^3(x_j - 1/2)\} + \{\sin(2\pi x_j) + 90/\pi^3(x_j - 1/2)\}.$$

The difference is because the $Beta(2, 2)$ distribution puts more weight into the center of the unit interval, which can best be understood graphically, see Figure 1.

Definition 2 (GAM with effect decomposition). Applying decomposition (5) to all additive components of a GAM, we obtain a *GAM with effect decomposition*, where the true additive predictor reads as follows

$$\eta^*(\mathbf{X}) = \beta_0^* + \sum_{j=1}^p \beta_j^* \tilde{X}_j + \sum_{j=1}^p f_{j,nonlin}^*(X_j). \quad (6)$$

Thereby, $\tilde{X}_j = (X_j - \mathbb{E}[X_j])/\sqrt{\text{Var}(X_j)}$ is the standardized linear function and the true nonlinear effects $f_{j,nonlin}^*$ are subject to $\mathcal{L}^2(\mathbb{P}^{X_j})$ -orthogonality constraints of the form

$$\mathbb{E}[f_{j,nonlin}^*(X_j)] = 0 \quad \text{and} \quad \mathbb{E}[f_{j,nonlin}^*(X_j)X_j] = 0, \quad j = 1, \dots, p. \quad (7)$$

Remark 1. The natural counterpart of the constraints (7) is empirical orthogonality on the estimation side. Thus, the effect decomposition (5) has implicitly been used by several authors including Scheipl et al. (2012); Chouldechova and Hastie (2015); Rossell and Rubio (2023), but this has not been made precise. However, having a precise definition of the true linear and nonlinear effect is important for three reasons. First, having a precise definition allows us to establish a consistency result of the form $\hat{f}_{j,lin} \xrightarrow{\mathbb{P}} f_{j,lin}^*$ and $\hat{f}_{j,nonlin} \xrightarrow{\mathbb{P}} f_{j,nonlin}^*$ in Theorem 1. To this end, we exploit that the suggested decomposition (5) is closely related to the functional ANOVA decomposition of Stone (1994) and Huang (1998), where a multidimensional function is decomposed into main effects and interactions. This connection allows us to use high-level results from Huang (1998) to prove our consistency result. Second, we can compute effectwise root mean squared errors (RMSEs) and missclassification rates in simulation settings. For instance, if we supply the function $f_j^* = \sin(2\pi x_j)$ under a uniform design, we can compare the estimated linear

effect $\widehat{f}_{j,lin}$ with its true counterpart $f_{j,lin}^* = -6/\pi(x_j - 1/2)$ and similarly for the nonlinear effect. Consequently, and third, separate interpretation of $\widehat{f}_{j,lin}$ and $\widehat{f}_{j,nonlin}$ becomes possible.

For estimation, we expand the nonlinear effects in a new construction of the Demmler-Reinsch (DR) basis for P-splines. We detail this in the following together with a proof that the DR basis allows for consistent effect estimation in the GAM with effect decomposition (6).

2.1 A new construction of the DR basis for P-splines

Let X_j be a continuous covariate with realized vector $\mathbf{x}_j = (x_{1j}, \dots, x_{nj})^T$. The construction of the design matrix $\mathbf{Z}_j \in \mathbb{R}^{n \times d_j}$ is based on the following three steps:

Algorithm 1: New DR basis for P-splines

1. **Set up the P-spline design:** Set up the B-spline design matrix $\mathbf{B}_j \in \mathbb{R}^{n \times (d_j+2)}$ and the associated roughness penalty matrix $\mathbf{K}_j \in \mathbb{R}^{(d_j+2) \times (d_j+2)}$. By default, we use cubic B-splines ($m = 3$) with equidistant knots in the range of \mathbf{x}_j and a second order differences penalty matrix $\mathbf{K}_j = \mathbf{\Delta}_j^T \mathbf{\Delta}_j$ (see Appendix A for details).
 2. **Compute the transition matrix:** Set up the constraint matrix $\mathbf{C}_j = (\mathbf{1}_n, \mathbf{x}_j)^T \mathbf{B}_j \in \mathbb{R}^{2 \times (d_j+2)}$ and compute a singular value decomposition (SVD) of \mathbf{C}_j to obtain a basis $\mathbf{V}_{0,j}$ of the nullspace $\ker(\mathbf{C}_j)$. Compute $\widetilde{\mathbf{K}}_j = \mathbf{V}_{0,j}^T \mathbf{K}_j \mathbf{V}_{0,j}$, $\widetilde{\mathbf{G}}_j = \mathbf{V}_{0,j}^T (\mathbf{B}_j^T \mathbf{B}_j / n) \mathbf{V}_{0,j} \in \mathbb{R}^{d_j \times d_j}$ and solve the generalized eigenvalue problem (Parlett, 1998, Chapter 15) for the pair of matrices $(\widetilde{\mathbf{G}}_j, \widetilde{\mathbf{K}}_j)$. Define \mathbf{A}_j as the matrix of columnwise generalized eigenvectors and the transition matrix $\mathbf{T}_j = \mathbf{V}_{0,j} \mathbf{A}_j$.
 3. **Perform the change-of-basis:** Set $\mathbf{Z}_j = \mathbf{B}_j \mathbf{T}_j$. Optionally rescale \mathbf{Z}_j by a positive scalar, such that $\text{trace}(\mathbf{Z}_j^T \mathbf{Z}_j / n) = 1$ and adjust \mathbf{T}_j accordingly.
-

The resulting basis functions are empirically orthogonal in the sense that $\mathbf{Z}_j^T \mathbf{Z}_j$ is diagonal, and the corresponding roughness penalty matrix is a scalar multiple of the identity matrix \mathbf{I}_{d_j} . In addition, $(\mathbf{1}_n, \mathbf{x}_j)^T \mathbf{Z}_j = \mathbf{0}$, which will be shown to be essential for consistent effect estimation in the subsequent Section 2.2. Figure 2 illustrates the resulting basis functions for a uniform and an exponential covariate design.

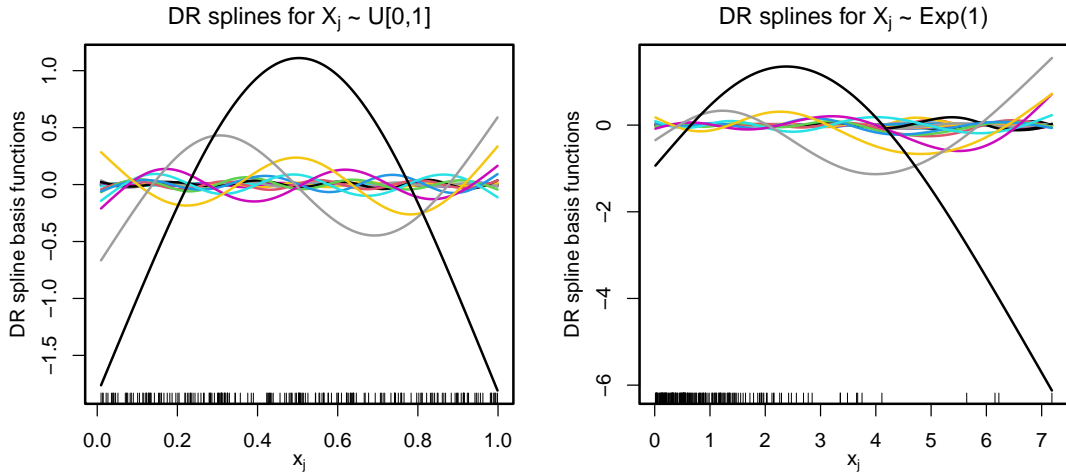


Figure 2: Illustration DR basis. Shown are $d_j = 25$ DR spline basis functions for $n = 200$ uniformly (left) and exponentially distributed design points x_{ij} (right).

Remark 2. The present construction of the DR basis has three major advantages compared to existing suggestions in the literature:

1. It is less restrictive than the approaches of [Nychka and Cummins \(1996\)](#); [Ruppert \(2002\)](#); [Claeskens et al. \(2009\)](#); [Wood \(2017\)](#); [He and Wand \(2023\)](#), which all require \mathbf{B}_j to have full rank. In contrast, \mathbf{B}_j can be rank-deficient for the present construction. This is important as \mathbf{B}_j is occasionally rank-deficient in applications when using P-splines with equidistant knots. Following a classical result by [Schoenberg and Whitney \(1953\)](#), the spline knots and the covariate values x_{ij} , $i = 1, \dots, n$, need to satisfy an interlacing condition for \mathbf{B}_j to have full rank, which is not always satisfied in practice (see also [de Boor, 2001](#), Chapter 14). We only require that $(\mathbf{1}_n, \mathbf{x}_j)$ has full rank, which is already the case if there exist two distinct covariate values.
2. The present construction is much more efficient than the approach of [Scheipl et al. \(2012\)](#), which relies on a truncated SVD of the implied $n \times n$ prior covariance matrix $\mathbf{B}_j \mathbf{K}_j^+ \mathbf{B}_j^T$, where \mathbf{K}_j^+ denotes the Moore-Penrose pseudoinverse of \mathbf{K}_j . This is because we only need to factorize matrices of sizes $2 \times (d_j + 2)$ and $d_j \times d_j$, whereas [Scheipl et al. \(2012\)](#) need to handle a matrix of size $n \times n$, and usually $d_j \ll n$ for P-splines ([Eilers and Marx, 1996](#)). In addition, the transition matrix \mathbf{T}_j is directly available for the present approach facilitating predictions at test points, which is rather cumbersome for [Scheipl et al. \(2012\)](#).

3. Algorithm 1 is general in the sense that it can also be applied for P-splines of a different spline degree ($m \geq 1$) or other types of penalized splines such as O’Sullivan penalized splines with integrated squared second derivative as roughness penalty (O’Sullivan, 1986; Wand and Ormerod, 2008). In addition, the underlying ideas can also be used to construct suitable design matrices for spatial effects (for both discrete and continuous spatial data; see Appendix C.2 for details).

2.2 Consistent effect estimation using the DR basis

Stone (1986) establishes a general consistency result for the maximum likelihood additive spline estimator in the GAM (1). It is shown that if certain regularity conditions are satisfied, then the estimated additive components \hat{f}_j converge to their true counterparts f_j^* , that is, $\|\hat{f}_j - f_j^*\|_j \xrightarrow{\mathbb{P}} 0$ as $n \rightarrow \infty$, where $\|\cdot\|_j$ denotes the $\mathcal{L}^2(\mathbb{P}^{X_j})$ -norm. To support the suitability of the DR basis for estimation in the GAM with effect decomposition (6), we next extend the result of Stone (1986) to the present situation.

Theorem 1 (Consistency). Assume that the regularity conditions of Theorem 2 in Stone (1986) hold with spline degree $m \geq 1$. Let the additive components used for maximization of the likelihood have the form $f_j = f_{j,lin} + f_{j,nonlin} = \tilde{x}_j \beta_j + \sum_{l=1}^{d_j} \phi_{j,l} u_{j,l}$ with DR basis functions $\phi_{j,l}$, $l = 1, \dots, d_j$, for the nonlinear effects. Then it holds:

$$\|\hat{f}_{j,lin} - f_{j,lin}^*\|_j \xrightarrow{\mathbb{P}} 0 \quad \text{and} \quad \|\hat{f}_{j,nonlin} - f_{j,nonlin}^*\|_j \xrightarrow{\mathbb{P}} 0,$$

for $j = 1, \dots, p$, as $n \rightarrow \infty$.

A proof of Theorem 1 is provided in Appendix B.

Remark 3. Theorem 1 shows that consistent estimation of the true linear and nonlinear effects in the GAM with effect decomposition (6) is feasible when using the DR basis from Algorithm 1 to model the nonlinear effects. Owing to the generality of the result of Stone (1986), Theorem 1 holds for several conditional response families $Y \mid \mathbf{X}$ including a Gaussian, logistic or Poisson additive model. The proof of Theorem 1 is not trivial as the effect decomposition of \hat{f}_j is based on the empirical covariate distribution $\mathbb{P}_n^{X_j} = 1/n \sum_{i=1}^n \delta_{X_{ij}}$, while the decomposition of f_j^* is based on its theoretical counterpart \mathbb{P}^{X_j} . This leads to similar challenges as in the study of

empirical processes (van de Geer, 2000), and we use a general result from Huang (1998) to show that the empirical semi-inner product and its theoretical counterpart are uniformly close on the approximating sieve of spline spaces (see Appendix B for details).

2.3 Comparison of DR basis and MMR

To demonstrate the practical relevance of Theorem 1, we next compare the DR basis and the commonly used MMR of Fahrmeir et al. (2004) in an illustrative example (see Appendix C.1 for details on the MMR and the closely related Euler’s transformation). For conciseness, we limit the presentation to the most relevant aspects, further details on the comparison are provided in Appendix C.3. Consider the model

$$Y_i = f^*(X_i) + \epsilon_i, \quad \epsilon_i \stackrel{iid}{\sim} N_1(0, \sigma^2),$$

with $X_i \stackrel{iid}{\sim} U[0, 1]$ and $f^*(x) = \sin(2\pi x) + (x - 1/2)$, as well as $\sigma^2 = 1$ and $n = 500$. For estimation, we use a predictor of the form (4) with $p = 1$, where we use either the DR basis or the MMR for the design matrix \mathbf{Z} of the nonlinear effect.

Figure 3 depicts the resulting estimates across $R = 50$ replicates. We see that the DR basis and the MMR perform equally well for estimation of the overall effect f^* . However, the MMR does not perform well in estimating the true linear and nonlinear effects separately. In fact, both effect estimates are highly biased for the MMR. The reason is that $(\mathbf{1}_n, \mathbf{x})^T \mathbf{Z} = \mathbf{0}$ for the DR basis but not for the MMR. In Appendix C.3 we conduct several additional analyses showing inter alia that the bias for the MMR persists as n increases and that Euler’s transformation (the default in the popular R package `mboost`) leads to similar problems. In general, we conclude that empirical orthogonality, i.e. $(\mathbf{1}_n, \mathbf{x}_j)^T \mathbf{Z}_j = \mathbf{0}$, is crucial to achieve satisfactory estimation performance in the GAM with effect decomposition (6).

3 Bayesian Effect Selection

In this section we combine the DR basis with a Bayesian group selection prior to perform data-driven effect selection. We consider a GAM with effect decomposition (6) and a potentially large number of continuous covariates p . We assume *effect sparsity*, that is, we assume that

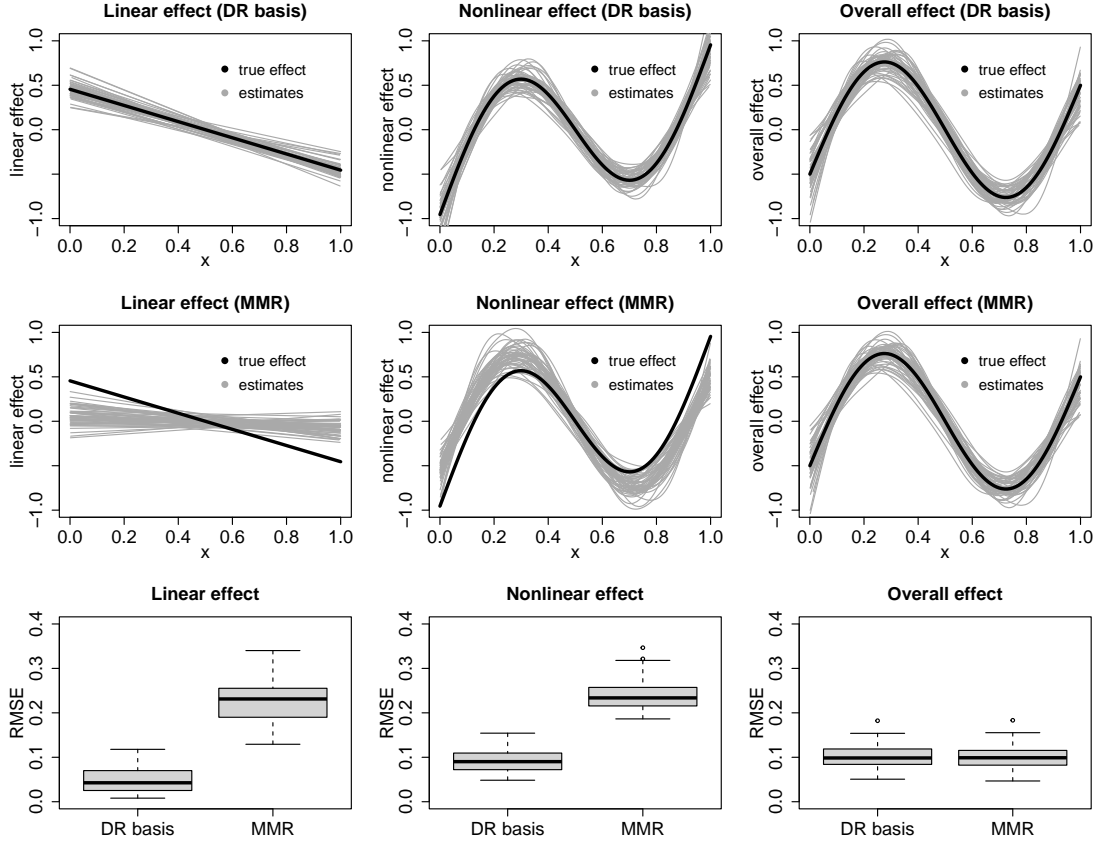


Figure 3: Comparison of DR basis and MMR. Shown are the linear/nonlinear/overall effect estimates (first/second/third column), across the $R = 50$ replicate data sets when using the DR basis (first row) or the MMR (second row) to model the nonlinear effect. The solid black lines show the true linear, nonlinear and overall effect according to Definition 1. The third row shows the corresponding effectwise RMSEs.

only some of the covariates have a linear effect ($\beta_j^* \neq 0$) and only some of the covariates have a nonlinear effect ($f_{j,nonlin}^* \neq 0$). Some of the covariates may have no effect on the response at all ($\beta_j^* = 0, f_{j,nonlin}^* = 0$).

Our goal is to perform effect selection, that is, we aim to develop a framework that allows to detect automatically (i.e. in a data driven manner) whether a linear or a nonlinear effect of a continuous covariate are present or not. To facilitate the exposition, we first introduce a new notation for the vector of predictor evaluations (4). In the following we write

$$\boldsymbol{\eta} = \beta_0 \mathbf{1}_n + \sum_{j=1}^J \boldsymbol{\psi}_j \boldsymbol{\beta}_j = \beta_0 \mathbf{1}_n + \boldsymbol{\psi} \boldsymbol{\beta}, \quad (8)$$

where the $\boldsymbol{\psi}_j$ are generic design matrices of sizes $n \times d_j$ and the $\boldsymbol{\beta}_j \in \mathbb{R}^{d_j}$ are coefficient vectors to be estimated. Thereby, $\boldsymbol{\psi}_j = \tilde{\boldsymbol{x}}_j$ for a linear effect and $\boldsymbol{\psi}_j = \mathbf{Z}_j$ from Algorithm 1 for a nonlinear effect. Moreover, $\boldsymbol{\psi} = (\boldsymbol{\psi}_1, \dots, \boldsymbol{\psi}_J)$ and $\boldsymbol{\beta} = (\boldsymbol{\beta}_1^T, \dots, \boldsymbol{\beta}_J^T)^T$. In terms of (8), effect sparsity simply corresponds to group sparsity, that is, we assume that $\boldsymbol{\beta}_j = \mathbf{0}$ for some of the $j \in \{1, \dots, J\}$. Many different approaches such as penalized likelihood or boosting can be used to tackle the resulting group selection problem. In this paper, we opt for a fully Bayesian approach with MCMC sampling. To this end, we endow the $\boldsymbol{\beta}_j$ with the recently proposed normal beta prime spike and slab (NBPSS) prior of Klein et al. (2021).

3.1 Normal beta prime spike and slab prior

We introduce positive variance parameters τ_j^2 and binary selection indicators $\gamma_j \in \{0, 1\}$ as well as effect-specific weights $\omega_j \in (0, 1)$. Following Klein et al. (2021) we use a prior of the form

$$\begin{aligned} \boldsymbol{\beta}_j \mid \tau_j^2 &\sim N_{d_j}(\mathbf{0}, \tau_j^2 \mathbf{I}_{d_j}) \\ \tau_j^2 \mid \gamma_j &\sim SBP(a_j, b_j, c_j, \gamma_j), \\ \gamma_j \mid \omega_j &\sim Bernoulli(\omega_j), \\ \omega_j &\sim Beta(a_{\omega_j}, b_{\omega_j}), \end{aligned} \quad (9)$$

for $j = 1, \dots, J$, with scale parameters $c_{j,0} \ll c_{j,1}$ for the spike and the slab, respectively. Above, $SBP(a, b, c)$ denotes the scaled beta prime distribution with shape parameters a and b and scale parameter c whose density function is

$$SBP(x; a, b, c) = 1/(c B(a, b)) (x/c)^{(a-1)} (1 + x/c)^{-(a+b)}, \quad x > 0,$$

where $B(a, b)$ is the beta function (see Pérez et al., 2017, for details). To complete the prior specification, we place an improper uniform prior $p(\beta_0) \propto 1$ on the intercept and a suitable prior on the dispersion parameter if present (e.g., Jeffreys’ prior $p(\sigma^2) \propto 1/\sigma^2$ in the Gaussian model).

3.2 Prior hyperparameters

We follow Klein et al. (2021) and use $a_j = 1/2$ and $b_j = 5$ for the shape parameters of the scaled beta prime distribution. To elicit suitable values for the scale parameters $c_{j,0}$ and $c_{j,1}$, we use a prior scaling approach. The key idea is to choose $c_{j,0}$ and $c_{j,1}$ such that prior effect draws $\mathbf{f}_j = \psi_j \beta_j$ from both, the spike and the slab have a reasonable size (see Appendix E.2 for details). For the ω_j we use uniform priors with $a_{\omega_j} = b_{\omega_j} = 1$ by default. Our implementation also supports a global ω , which may allow for better adaption to the unknown sparsity level in high-dimensional settings (Ročková, 2018; Bai et al., 2022).

3.3 Posterior inference

Effect selection and estimation is based on the posterior distribution, which by Bayes’ rule, has density proportional to

$$p(\beta_0, \boldsymbol{\beta}, \boldsymbol{\tau}^2, \boldsymbol{\gamma}, \boldsymbol{\omega} \mid \mathcal{D}) \propto p(\mathcal{D} \mid \beta_0, \boldsymbol{\beta}) \prod_{j=1}^J p(\boldsymbol{\beta}_j \mid \tau_j^2) p(\tau_j^2 \mid \gamma_j) p(\gamma_j \mid \omega_j) p(\omega_j),$$

where $\boldsymbol{\tau}^2 = (\tau_1^2, \dots, \tau_J^2)^T$, $\boldsymbol{\gamma} = (\gamma_1, \dots, \gamma_J)^T$ and $\boldsymbol{\omega} = (\omega_1, \dots, \omega_J)^T$. As the posterior is analytically intractable, we use MCMC to sample from it. A schematic overview of our sampler is shown in Algorithm 2, further details are provided in Appendix E.3.

Algorithm 2: Schematic MCMC sampler for NBPSS

For $t = 1, \dots, T$:

- Sample $\boldsymbol{\beta}^{(t)}$ using a Metropolis-Hastings step with IWLS proposal (Gamerman, 1997).
 - For $j = 1, \dots, J$: Sample $(\tau_j^2)^{(t)}$ using a slice step (Neal, 2003).
 - For $j = 1, \dots, J$: Sample $\gamma_j^{(t)}$ using a Gibbs step.
 - For $j = 1, \dots, J$: Sample $\omega_j^{(t)}$ using a Gibbs step.
-

3.4 Effect selection and estimation

We use the marginal posterior inclusion probabilities $\mathbb{P}(\gamma_j = 1 \mid \mathcal{D})$ for effect selection. Specifically, we say that the j -th effect $\mathbf{f}_j = \boldsymbol{\psi}_j \boldsymbol{\beta}_j$ is present if $\mathbb{P}(\gamma_j = 1 \mid \mathcal{D}) \geq 0.5$, which corresponds to the median probability model (Barbieri and Berger, 2004; Barbieri et al., 2021). For effect estimation, we use the marginal posterior mean $\hat{\mathbf{f}}_j = \boldsymbol{\psi}_j \hat{\boldsymbol{\beta}}_j$ with $\hat{\boldsymbol{\beta}}_j = \mathbb{E}[\boldsymbol{\beta}_j \mid \mathcal{D}]$, and for uncertainty quantification we use 95% posterior credible intervals (pointwise, equal-tailed).

3.5 MCMC mixing of the binary selection indicators

It is well-known that MCMC mixing of the binary selection indicators γ_j is notoriously difficult for Bayesian group selection approaches, especially if the group dimensions $d_j = \dim(\boldsymbol{\beta}_j)$ are not small (cf., Scheipl et al., 2012; Klein et al., 2021; Wiemann et al., 2021). In the worst case, the MCMC sampler can get stuck in the spike $\gamma_j = 0$ or the slab $\gamma_j = 1$, leading to unreliable MCMC inference for the posterior inclusion probabilities $\mathbb{P}(\gamma_j = 1 \mid \mathcal{D})$. Following Scheipl et al. (2012), we approximate the $\mathbb{P}(\gamma_j = 1 \mid \mathcal{D})$ using the average of the conditional posterior inclusion probabilities $1/T \sum_{t=1}^T \mathbb{P}(\gamma_j^{(t)} = 1 \mid \cdot)$ instead of the average of the indicators $1/T \sum_{t=1}^T \gamma_j^{(t)}$. This corresponds to Rao-Blackwellization, which is usually slightly more efficient (Robert and Roberts, 2021). We investigate the accuracy of the Rao-Blackwellized MCMC approximation in Appendix E.4. In line with the findings of Klein et al. (2021), we observe that MCMC mixing is very satisfactory for NBPSS, even for large dimensional groups. For comparison, we also investigate the mixing when using the popular SSGL prior of Bai et al. (2022) as a potential alternative to the NBPSS prior, but we find that NBPSS generally yields much better MCMC mixing. In the following Section 4 we establish new theoretical results, which may explain the favorable MCMC mixing of NBPSS compared to the SSGL.

4 Theoretical Results

In this section we derive the following new theoretical results for the NBPSS prior.

1. A closed form representation for the marginal spike $p(\boldsymbol{\beta}_j \mid \gamma_j = 0)$ and slab $p(\boldsymbol{\beta}_j \mid \gamma_j = 1)$ of the group coefficient vector $\boldsymbol{\beta}_j \in \mathbb{R}^{d_j}$ with variance parameter τ_j^2 integrated out.

2. The implied spike $p(r_j | \gamma_j = 0)$ and slab $p(r_j | \gamma_j = 1)$ of the Euclidean norm $r_j = \|\beta_j\|_2$.

The implied spike and slab of the Euclidean norm are particularly interesting as they allow us to visualize the NBPSS prior for arbitrary group dimension $d_j \in \mathbb{N}$, while the marginal spike and slab can only be plotted for $d_j \in \{1, 2\}$.

4.1 Marginal spike and slab

To derive the marginal spike and slab, we need to compute the integral

$$\begin{aligned} p(\beta | \gamma) &= \int_0^\infty N_d(\beta; \mathbf{0}, \tau^2 \mathbf{I}_d) SBP(\tau^2; a, b, c_\gamma) d\tau^2 \\ &= \frac{1}{(2\pi)^{d/2} c_\gamma B(a, b)} \int_0^\infty (\tau^2)^{-d/2} \exp(-\|\beta\|_2^2 / (2\tau^2)) (\tau^2 / c_\gamma)^{a-1} (1 + \tau^2 / c_\gamma)^{-(a+b)} d\tau^2, \end{aligned}$$

where we omit the group index $j \in \{1, \dots, J\}$ to simplify the notation. [Hernández-Lobato et al. \(2013\)](#) refer to the density for the special case $a = b = 1/2$ as *group horseshoe* density and write that it is not possible to evaluate the above integral in closed form. [Klein et al. \(2021\)](#) use numerical integration to compute and visualize $p(\beta | \gamma)$ for $d \in \{1, 2\}$. Proposition 4.1 contradicts [Hernández-Lobato et al. \(2013\)](#) and provides a closed-form expression for $p(\beta | \gamma)$.

Proposition 4.1 (Marginal spike and slab).

$$p(\beta | \gamma) = \frac{\Gamma(b + d/2)}{(2\pi c_\gamma)^{d/2} B(a, b)} \mathcal{U}(b + d/2, -a + d/2 + 1, \|\beta\|_2^2 / (2c_\gamma)), \quad \beta \in \mathbb{R}^d, \quad (10)$$

where \mathcal{U} is Kummer's U function (see, e.g., [Abramowitz and Stegun, 1972, Chapter 13](#)).

A proof of Proposition 4.1 is provided in Appendix D.1.

Remark 4. [Armagan et al. \(2013\)](#) state the density (10) for the univariate case ($d = 1$). They refer to it as *horseshoe-like* but do not provide a derivation. A derivation for the univariate case can be found in [Aguilar and Bürkner \(2023\)](#). Proposition 4.1 generalizes this result to arbitrary dimension $d \in \mathbb{N}$ and we refer to the density (10) and the corresponding distribution as *group horseshoe-like*. Figure 4 shows an illustration for the univariate case $d = 1$.

4.2 Implied spike and slab of the norm

Next, we derive the implied spike and slab of the Euclidean norm $r = \|\beta\|_2$, which will allow us to visualize the NBPSS prior for arbitrary group dimension $d \in \mathbb{N}$. To this end, we use a general

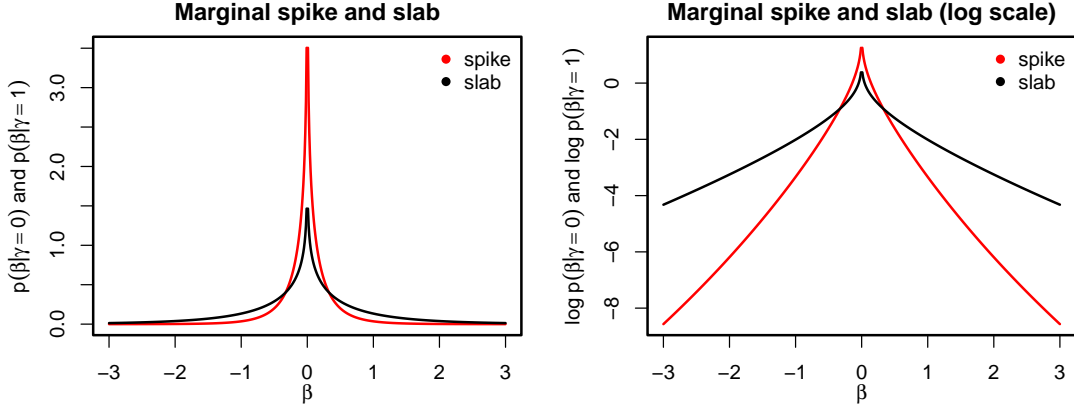


Figure 4: Theoretical results I. Shown are the marginal spike and slab (10) for $d = 1$ on the original scale (left) and the log scale (right). To evaluate Kummer's U function we use the R package `reticulate`, allowing us to access the function `hyperu` in the Python module `scipy.special`.

result from (Kelker, 1970, Section 5) for spherical distributions. With this, we obtain

Proposition 4.2 (Spike and slab of the norm).

$$p(r | \gamma) = \frac{2 \Gamma(b + d/2)}{(2c_\gamma)^{d/2} \Gamma(d/2) B(a, b)} r^{d-1} \mathcal{U}(b + d/2, -a + d/2 + 1, r^2/(2c_\gamma)), \quad r > 0.$$

A proof of Proposition 4.2 is provided in Appendix D.2. The implied spike and slab of the norm have the following properties.

Proposition 4.3 (Properties of the spike and slab of the norm).

i) The expected value is

$$\mathbb{E}[r | \gamma] = \int_0^\infty r p(r | \gamma) dr = \sqrt{2c_\gamma} \frac{B(a + 1/2, b - 1/2) \Gamma((d + 1)/2)}{B(a, b) \Gamma(d/2)}$$

for $b > 1/2$ and $+\infty$ for $b \leq 1/2$.

ii) The tail decay is controlled by the parameter b and it holds $p(r | \gamma) = O(r^{-(2b+1)})$ as $r \rightarrow \infty$.

iii) The behavior at the origin is controlled by the parameter a and it holds:

$$\lim_{r \rightarrow \infty} p(r | \gamma) = \begin{cases} \infty, & a \leq 1/2 \\ \kappa_1, & a > 1/2 \end{cases} \quad \text{and} \quad \lim_{r \rightarrow \infty} p(r | \gamma) = \begin{cases} \infty, & a < 1/2 \\ \kappa_2, & a = 1/2 \\ 0, & a > 1/2 \end{cases},$$

for $d = 1$ and $d > 1$ respectively, where $\kappa_1, \kappa_2 \in (0, \infty)$ are finite positive constants.

A proof of Proposition 4.3 is provided in Appendix D.3.

Figure 5 shows the implied spike and slab of the Euclidean norm for our choice of shape parameters $a = 1/2$ and $b = 5$ for a one-dimensional group ($d = 1$) and a ten-dimensional group ($d = 10$). The scale parameters c_0 and c_1 were chosen such that $\mathbb{E}[r \mid \gamma = 0] = 0.1$ and $\mathbb{E}[r \mid \gamma = 1] = 1$. For comparison, we also show the implied spike and slab of the norm for the SSGL prior of Bai et al. (2022). In that case the marginal spike and slab are group lasso densities of the form $p(\beta \mid \gamma) \propto \exp(-\lambda_\gamma \|\beta\|_2)$, $\beta \in \mathbb{R}^d$, and the implied spike and slab of the norm are gamma densities of the form $p(r \mid \gamma) \propto r^{d-1} \exp(-\lambda_\gamma r)$, $r > 0$. For the behavior at the origin it holds $\lim_{r \rightarrow 0} p(r \mid \gamma) = \lambda_\gamma$ for $d = 1$ and $\lim_{r \rightarrow 0} p(r \mid \gamma) = 0$ for $d > 1$.

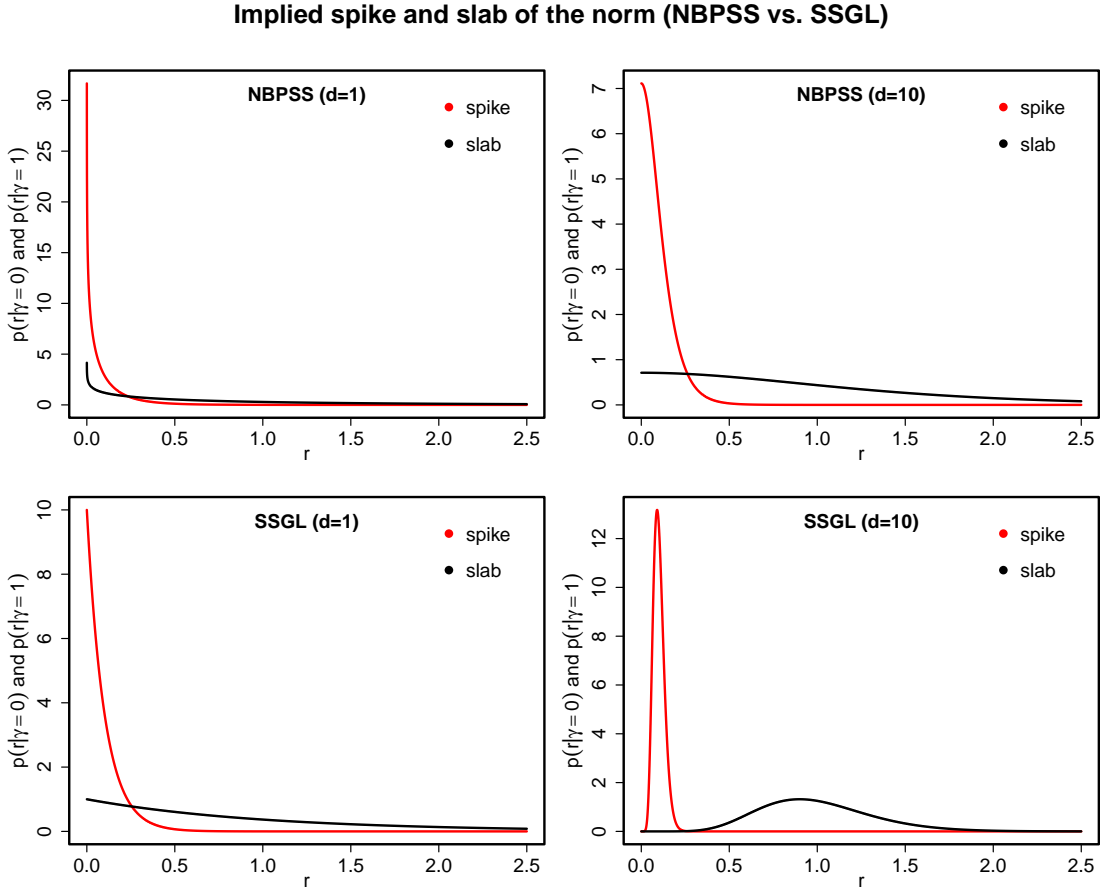


Figure 5: Theoretical results II. Shown are the implied spike and slab of the Euclidean norm for the NBPSS prior (top panel) and the SSGL prior (bottom panel). On the left we have $d = 1$ and on the right we have $d = 10$. The scale parameters were chosen such that $\mathbb{E}[r \mid \gamma = 0] = 0.1$ and $\mathbb{E}[r \mid \gamma = 1] = 1$ for each plot.

Remark 5. The implied spike and the slab of the Euclidean norm clearly overlap for NBPSS. This is true for both $d = 1$ and $d = 10$. For the SSGL, in contrast, the implied spike and the slab of the norm only overlap for $d = 1$ but not for $d = 10$. The reason is that the norm of the group lasso distribution concentrates sharply around d/λ_γ as the group dimension d grows. This behavior is somewhat similar to the concentration of the norm of a multivariate Gaussian distribution (Vershynin, 2018, Chapter 3). The group horseshoe-like distribution, in contrast, does not exhibit a similar behavior, provided that $a \leq 1/2$. To the best of our knowledge, this difference has not been highlighted in the literature before.

In Appendix E.4 we investigate the MCMC mixing of the binary selection indicators γ_j for both NBPSS and the SSGL and find that mixing is generally much better for NBPSS. We conjecture that the superior mixing of NBPSS can be explained by Figure 5. This is plausible because a sufficient overlap of the spike and the slab is also necessary to achieve good MCMC mixing in the context of Bayesian variable selection (George and McCulloch, 1993, 1997).

5 Application to Time-to-Event Data

In this section we illustrate the applicability of NBPSS for time-to-event data. Time-to-event data is very common in medical studies and the Cox model (Cox, 1972) is one of the most popular regression models in this context (George et al., 2014). Thereby, the covariates are linked to the hazard rate of the time-to-event response and in addition to categorical and continuous covariates, often also spatial information like the district or the exact place of residence of the study participants is available (Hennerfeind et al., 2006). While many approaches for estimation of flexible geoaddivitive Cox regression models are available (e.g. Martino et al., 2011; Wood, 2017; Zhou et al., 2020; Brilleman et al., 2020), only few allow for data-driven effect selection. One approach that is capable of effect selection in the geoaddivitive Cox model is model-based boosting (Hofner et al., 2014). In what follows, we first extend the geoaddivitive Cox model of Hennerfeind et al. (2006) to include our effect decomposition (6). Then, we conduct simulations comparing the performance of NBPSS and model-based boosting before considering an application on survival with leukemia.

5.1 The geoadditive Cox model with effect decomposition

Suppose we have data $\mathcal{D} = \{(t_i, \delta_i, \mathbf{v}_i), i = 1, \dots, n\}$, where $t_i \geq 0$ are time points, the $\delta_i \in \{0, 1\}$ are binary event indicators ($\delta_i = 1$ means that the event has occurred), and the $\mathbf{v}_i \in \mathbb{R}^p$ comprise realized covariate information of mixed type (binary, continuous, spatial) of \mathbf{V} . Without loss of generality we assume that categorical covariates are represented through dummy variables. Similar to [Hemmerfeind et al. \(2006\)](#), we assume that the conditional hazard rate has the form

$$h^*(t \mid \mathbf{V}) = \exp(g_0^*(t) + \eta^*(\mathbf{V})).$$

Thereby, the log baseline hazard rate $g_0^*(\cdot)$ is an unknown smooth function of time and $\eta^*(\mathbf{V})$ is a geoadditive predictor of the form

$$\eta^*(\mathbf{V}) = \sum_{j=1}^{p_d} \alpha_j^* D_j + \sum_{j=1}^{p_c} \beta_j^* \tilde{X}_j + \sum_{j=1}^{p_c} f_{j, \text{nonlin}}^*(X_j) + f_{\text{spat}}^*(\mathbf{S}), \quad (11)$$

with identifiability constraints $\mathbb{E}[f_{j, \text{nonlin}}^*(X_j)] = \mathbb{E}[f_{j, \text{nonlin}}^*(X_j)X_j] = 0$, $j = 1, \dots, p_c$, as well as $\mathbb{E}[f_{\text{spat}}^*(\mathbf{S})] = 0$. Some remarks are in order.

- The predictor η^* contains no intercept β_0^* since the overall level is covered through g_0^* .
- The D_j , $j = 1, \dots, p_d$, are dummy variables with values in $\{0, 1\}$.
- The functional effects of the continuous covariates X_j , $j = 1, \dots, p_c$, are decomposed into a linear and a nonlinear effect as in (6).
- The rightmost term $f_{\text{spat}}^*(\mathbf{S})$ is a spatial effect for either continuous data $\mathbf{S} \in \Omega \subseteq \mathbb{R}^2$ or discrete regional data $\mathbf{S} \in \{1, \dots, R\}$.

Crucially, we again assume effect sparsity, that is, we assume that some of the terms in (11) are negligible. Our goals are twofold: We want to identify the active effects and estimate them.

5.2 Estimation

For estimation, we expand the nonlinear effects and the spatial effect in DR bases (see Algorithm 1 and Appendix C.2, respectively). For the dummy variables we use the raw covariates and for the linear effects we use empirically standardized linear functions (as before). For the vector of predictor evaluations we can thus write $\boldsymbol{\eta} = \sum_{j=1}^J \boldsymbol{\psi}_j \boldsymbol{\beta}_j = \boldsymbol{\psi} \boldsymbol{\beta}$, where $J = p_d + 2 \times p_c + 1$

is the overall number of effects. Following [Hennerfeind et al. \(2006\)](#) we use cubic Bayesian P-splines ([Lang and Brezger, 2004](#)) to model the log baseline hazard rate $g_0(\cdot)$. Thus, we can write $\mathbf{g}_0 = \boldsymbol{\psi}_0 \boldsymbol{\beta}_0$ for the corresponding vector of function evaluations. With the usual assumptions about noninformative censoring, the full likelihood is

$$p(\mathcal{D} \mid \boldsymbol{\beta}_0, \boldsymbol{\beta}) = \prod_{i=1}^n h(t_i \mid \mathbf{v}_i)^{\delta_i} \exp\left(-\int_0^{t_i} h(u \mid \mathbf{v}_i) du\right).$$

To reflect our sparsity assumption, we endow the regression coefficients $\boldsymbol{\beta} = (\boldsymbol{\beta}_1^T, \dots, \boldsymbol{\beta}_J^T)^T$ with the NBPSS prior (9). In Appendix E.1 we derive the gradient and Hessian of the log-likelihood, which we need for efficient posterior sampling (see Appendix E.3). As the resulting expressions contain analytically intractable integrals, we cannot evaluate them directly but need to resort to numerical approximations (see Appendix E.1.2).

5.3 Numerical experiments

To investigate the performance of NBPSS in the geoadditive Cox model (11), we compare our method with the boosting approach of [Hofner et al. \(2014\)](#) as implemented in the R package `mboost`. To the best of our knowledge, this is the only directly available approach allowing for data-driven selection of linear, nonlinear and spatial effects in the geoadditive Cox model. The following two questions are of particular interest: 1. Does the DR basis lead to better selection and estimation performance than the MMR or Euler’s transformation? 2. Can `mboost` also benefit from using the DR basis? To answer the second question we use the flexibility of `mboost` to create new base-learners.

Simulation setting Following [Hennerfeind et al. \(2006\)](#) and to resemble our real data application in the subsequent Section 5.4, we consider the following data generating process:

- There are two dummy covariates D_1 and D_2 (each of them Bernoulli with mean 1/2) and eight continuous covariates X_1, \dots, X_8 (each of them uniform on $[0, 1]$). In addition, there is a two-dimensional spatial covariate \mathbf{S} , which is uniform on the unit square $[0, 1]^2$.
- The time points are generated from a Weibull distribution with shape parameter k and scale parameter $\exp(-\boldsymbol{\eta}^*(\mathbf{V})/k)$, that is, $T \mid \mathbf{V} \sim \text{Weibull}(k, \exp(-\boldsymbol{\eta}^*(\mathbf{V})/k))$, which

corresponds to the conditional log hazard rate $\log h^*(t | \mathbf{V}) = g_0^*(t) + \eta^*(\mathbf{V}) = \log k + (k - 1) \log t + \eta^*(\mathbf{V})$.

- The true geoadditive predictor η^* is

$$\eta^*(\mathbf{V}) = 0 \times D_1 + 1/2 \times D_2 + \sum_{j=1}^8 \beta_j^* \tilde{X}_j + \sum_{j=1}^8 f_{j,nonlin}^*(X_j) + f_{spat}^*(\mathbf{S}), \quad (12)$$

where $\tilde{X}_j = \sqrt{12}(X_j - 1/2)$ and $\boldsymbol{\beta}^* = (\beta_1^*, \dots, \beta_8^*)^T = (1/\sqrt{12}, -2/\sqrt{12}, 0, 0, \beta_5^*, -\sqrt{3}/\pi, 0, 0)^T$ with $\beta_5^* = -2\{5 + \exp(3)\}/\{3\sqrt{3}\exp(3)\}$. For the true nonlinear effects we use

$$\begin{aligned} - f_{1,nonlin}^* &= f_{2,nonlin}^* = f_{7,nonlin}^* = f_{8,nonlin}^* = 0, \\ - f_{3,nonlin}^* &= 4(x - 1/2)^2 - 1/3, \\ - f_{4,nonlin}^* &= f_{6,nonlin}^* = \sin(2\pi x) + 6/\pi(x - 1/2), \\ - f_{5,nonlin}^* &= 2 \exp(-3x) - \{2/3 - 2/3 \exp(-3)\} - \beta_5^* \sqrt{12}(x - 1/2). \end{aligned}$$

It is straightforward to verify that these satisfy the required identifiability constraints (7) (see Appendix F.1 for details and plots of the functions). For the spatial effect we set $f_{spat}^* \equiv 0$ so that there is no true spatial effect in η^* . With this, the true model has selection indicators $\boldsymbol{\gamma}^* = (0, 1 | 1, 1, 0, 0, 1, 1, 0, 0 | 0, 0, 1, 1, 1, 1, 0, 0 | 0)^T$, where we use the same order as in (12), i.e. we first have the two dummies, followed by the linear, nonlinear and spatial effects.

- We generate a sample of size $n = 1,000$ with Weibull shape $k = 3/2$ and censor the generated time points at $t_{cens} = 2$ leading to a censoring rate of about 14%.

Competitors and performance measures We generate $R = 100$ replicate data sets and apply NBPSS and `mboost` for estimation and effect selection. For both methods we consider three basis expansions based on Euler’s transformation, the MMR and the DR basis for the nonlinear effects of the continuous covariates. Throughout, we use $d_j = 9$ basis functions. Other choices such as $d_j \in \{14, 19\}$ led to slightly worse performance although the differences were minor. For NBPSS we use 1,000 MCMC iterations from which we discard the first 100 as burn-in. For `mboost` we use early stopping as recommended by Hofner et al. (2014). To this end, we first use 500 boosting iterations and then optimize the number of boosting iterations using 25 bootstrap samples. To judge the performance of NBPSS and `mboost` in the three different

variants, we compute effectwise missclassification rates $1/R \sum_{r=1}^R |\hat{\gamma}_j^{(r)} - \gamma_j^*|$, $j = 1, \dots, J$, as well as the overall RMSE $\|\hat{\boldsymbol{\eta}} - \boldsymbol{\eta}^*\|_2/\sqrt{n}$ at the observed covariates.

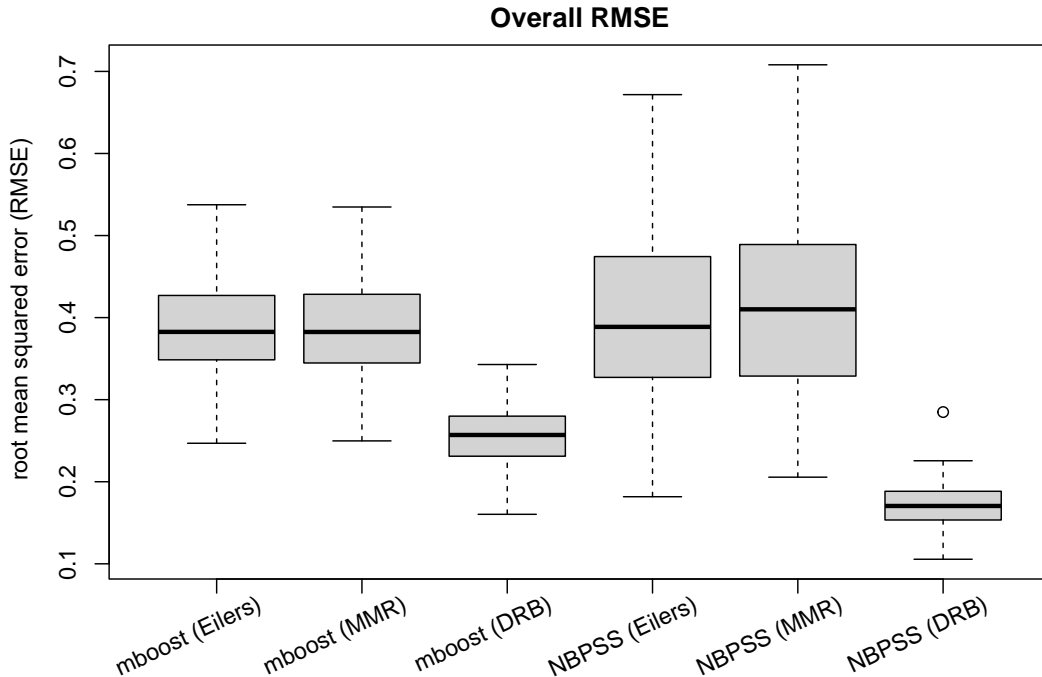


Figure 6: RMSEs. Shown is the overall RMSE $\|\hat{\boldsymbol{\eta}} - \boldsymbol{\eta}^*\|_2/\sqrt{n}$ for the different variants of `mboost` and `NBPSS` across the $R = 100$ replicates.

Results The results are shown in Figure 6 and Table 1. Overall, the DR basis yields the best performance for both methods, `NBPSS` and `mboost`. Using the DR basis, `NBPSS` outperforms `mboost` in terms of both, RMSE and selection accuracy. Closer inspection of Table 1 reveals that `mboost` tends to select overly complex models. This is in line with the literature and a current research topic (Mayr et al., 2023). While it is not surprising that the DR basis leads to lower effectwise missclassification rates, the large gains in overall RMSE are somewhat surprising but consistent across different settings. In Appendix F.2 we consider several other scenarios, where we include a true spatial effect in the predictor, vary the sample size $n \in \{100, 250, 500, 2000\}$ and introduce correlation among the continuous covariates X_j . The overall picture is well in line with the present results, and the combination of `NBPSS` and the DR basis consistently leads to the best performance.

Effect	D1	D2	L1	L2	L3	L4	L5	L6	L7	L8	N1	N2	N3	N4	N5	N6	N7	N8	S	Av.
Active	0	1	1	1	0	0	1	1	0	0	0	0	1	1	1	1	0	0	0	9/19
mboost (Eilers)	10	0	0	0	0	98	0	79	4	6	97	97	0	0	0	0	83	78	99	34
mboost (MMR)	11	0	0	0	0	97	0	80	5	5	97	97	0	0	0	0	84	75	97	34
mboost (DRB)	6	0	0	0	32	27	0	0	14	28	92	91	0	0	0	0	89	86	96	30
NBPSS (Eilers)	2	0	0	0	3	100	0	84	2	1	4	6	0	0	1	0	1	4	5	11
NBPSS (MMR)	3	0	0	0	2	100	0	79	2	0	8	6	0	0	3	0	1	2	6	11
NBPSS (DRB)	2	0	0	0	3	2	0	0	2	2	10	7	0	0	1	0	4	8	2	2

Table 1: Missclassification rates. Shown is the effectwise missclassification rate in percent across the $R = 100$ replicates. Rows refer to methods while columns refer to effects. The first row indicates the effect (D stands for dummy, L for linear, N for nonlinear and S for spatial). The second row indicates whether the effect is truly active ($\gamma_j^* = 1$) or not ($\gamma_j^* = 0$). The rightmost column shows rowwise averages and can be regarded as an overall measure of selection accuracy.

5.4 Illustration: survival with leukemia

To illustrate the practical usefulness of the developed methodology, we analyze the `LeukSurv` data set. The data set is contained in the R package `spBayesSurv` (Zhou et al., 2020) and has previously been analyzed by several different authors including Henderson et al. (2002); Kneib and Fahrmeir (2007); Lindgren et al. (2011); Zhou and Hanson (2018).

Model specification The data set contains survival information for $n = 1,043$ patients from Northwest England suffering from acute myeloid leukemia. About 16% of the survival times are right-censored and available covariates are the patient’s age (age), the white blood cell count at diagnosis (wbc), the Townsend deprivation index (tpi) as well as the patient’s sex (sex). In addition to that, the exact residential location of the patients is available ($space$). To contribute to a better understanding of the covariate effects, we consider the geoaddivitive Cox model

$$\log h(t_i | \mathbf{v}_i) = g_0(t_i) + \alpha sex_i + \beta_1 age_i + \beta_2 wbc_i + \beta_3 tpi_i + f_{age}(age_i) + f_{wbc}(wbc_i) + f_{tpi}(tpi_i) + f_{spat}(space_i), \quad i = 1, \dots, n.$$

We expand the nonlinear effects $f_{age}, f_{wbc}, f_{tpi}$ of the continuous covariates age, wbc and tpi in terms of DR spline bases as explained in Section 2.1. For the spatial effect f_{spat} we use tensor

product B-splines and a Kronecker sum penalty. Then, we apply a DR type reparametrization to realize the centering constraints and to obtain a multiple of the identity matrix as penalty matrix (see Appendix C.2 for details). For the log baseline hazard rate $g_0(\cdot)$ we use $d_0 = 10$ cubic Bayesian P-splines with second order differences penalty.

MCMC sampling We use $T = 50,000$ MCMC iterations and discard the first 10,000 as burn-in (overall runtime about 32 minutes). The MH acceptance rate for β_0 was about 30% and for β it was about 82%. Further MCMC diagnostics indicate that the sampler has converged to the desired target distribution (see Appendix F.3).

Results Figure 7 depicts the estimated log baseline hazard rate. We see that the hazard rate mainly decreases but sharply increases towards the end of the observation period. However, some caution is warranted as the observed time exceeds 10 years for only 26 patients. The estimated covariate and spatial effects are shown in Figures 8 and 9, respectively. Overall, the picture is well in line with the findings of Kneib and Fahrmeir (2007), who use an empirical Bayes approach for estimation and the Akaike information criterion (AIC) for model selection. Interestingly, Kneib and Fahrmeir (2007) fit a range of different models and conclude that the fully-nonparametric model with nonlinear effects for all continuous covariates performs best in terms of AIC, even though the overall effect of *wbc* appears to be linear from their plot too (as in our case). Using the posterior inclusion probabilities, we conclude that a linear effect should actually be sufficient for modeling *wbc*. We acknowledge, however, that the inclusion probability is fairly close to the threshold of 0.5 (see Figure 10).

6 Discussion and Conclusion

The main contribution of this paper is to highlight the importance of orthogonality between the linear and the nonlinear effect for efficiently estimating sparse partially linear additive models. Only then do we obtain consistent estimation of the true linear and nonlinear effect, which we define in terms of $\mathcal{L}^2(\mathbb{P}^{X_j})$ -projections. To achieve orthogonality, we expand the nonlinear effects in DR spline bases. We suggest a new construction of the DR basis for P-splines, which is more efficient and less restrictive than previous suggestions as it does not require full rank

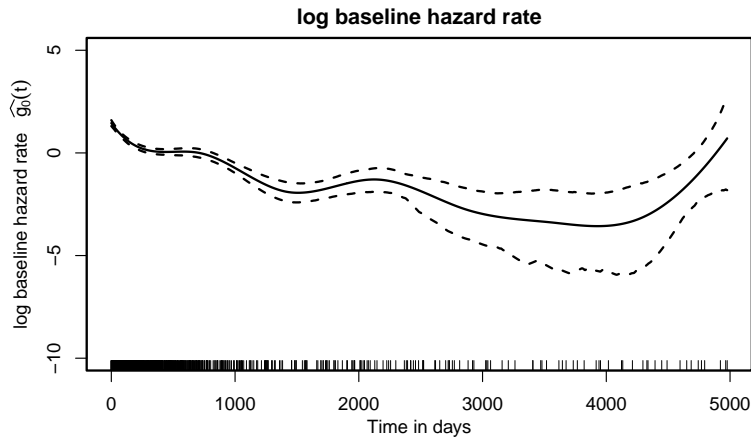


Figure 7: Survival with leukemia I. Estimated log-baseline hazard rate.

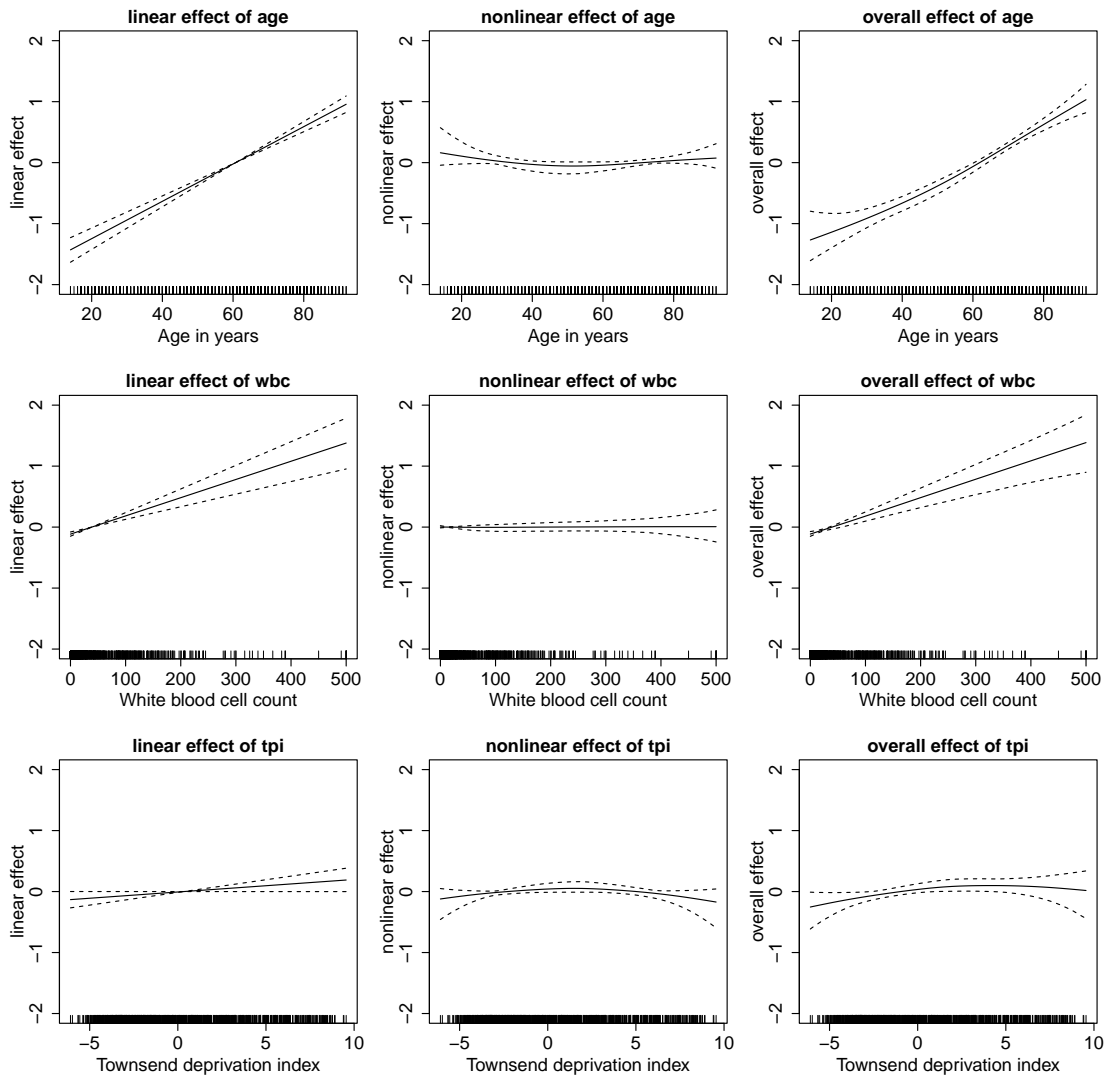


Figure 8: Survival with leukemia II. Estimated covariate effects.

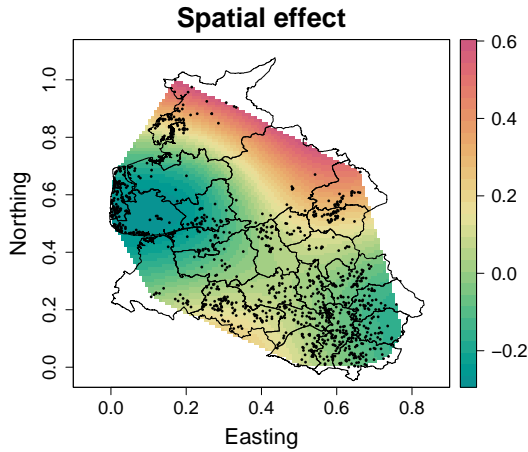


Figure 9: Survival with leukemia III.

Estimated spatial effect.

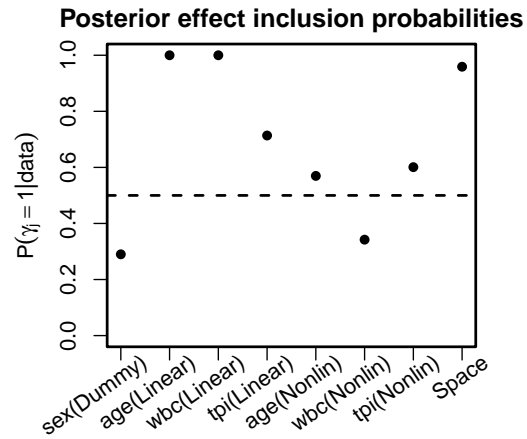


Figure 10: Survival with leukemia IV.

Estimated posterior inclusion probabilities.

of the B-spline design matrix. Thereby, our proposal can be seen as an attractive default for additive P-spline regression, irrespective of whether a Bayesian, boosting or penalized likelihood approach is used for estimation. Our simulations for the geoadditve Cox model show that the DR basis is not only theoretically but also empirically superior to the commonly used MMRs. Interestingly, not only our Bayesian method but also the boosting approach of [Hofner et al. \(2014\)](#) benefits from using the DR basis for the nonlinear effects.

Another important contribution of this work is that we allow for a better understanding of the superior MCMC mixing properties of the recently proposed NBPSS prior. To this end, we analytically derive and investigate the implied spike and slab of the Euclidean norm of the group coefficient vectors. In general, we argue that the implied prior density of the norm is a key quantity for Bayesian group selection approaches and should always be investigated and visualized.

Two promising directions for future research are as follows. First, as an alternative to the geoadditve Cox model, one may investigate Bayesian effect selection for parametric survival models such as a geoadditve Weibull regression model or a Weibull model with geoadditve predictors on both, the scale and the shape parameter. We have focused on the Cox model because it is still the most popular survival model in applications ([George et al., 2014](#)), but the investigation of parametric alternatives would be very interesting. Second, as a potential

alternative to MCMC, one may investigate Bayesian effect selection for non-standard likelihoods using faster approximate Bayesian methods such as variational inference. [He and Wand \(2023\)](#) provide such an option using a mean field approximation but their approach is limited to a Gaussian response model and a binary probit model, and it would definitely be interesting to broaden the scope in future research. For both of these directions it will be important to have an orthogonal decomposition and the suggested construction of the DR basis will be convenient to model the nonlinear effects of continuous covariates.

Acknowledgements

This work was funded by the Deutsche Forschungsgemeinschaft (DFG, German Research Foundation) through the Emmy Noether grant KL 3037/1-1.

References

- Abramowitz, M. and Stegun, I. A. (1972). *Handbook of Mathematical Functions with Formulas, Graphs, and Mathematical Tables*. US Government Printing Office, Washington, D.C. tenth printing.
- Aguilar, J. E. and Bürkner, P.-C. (2023). Intuitive joint priors for Bayesian linear multilevel models: The R2D2M2 prior. *Electronic Journal of Statistics*, 17(1):1711–1767.
- Armagan, A., Dunson, D. B., Lee, J., Bajwa, W. U., and Strawn, N. (2013). Posterior consistency in linear models under shrinkage priors. *Biometrika*, 100(4):1011–1018.
- Bai, R., Moran, G. E., Antonelli, J. L., Chen, Y., and Boland, M. R. (2022). Spike-and-slab group lassos for grouped regression and sparse generalized additive models. *Journal of the American Statistical Association*, 117(537):184–197.
- Barbieri, M. M. and Berger, J. O. (2004). Optimal predictive model selection. *The Annals of Statistics*, 32(3):870–897.
- Barbieri, M. M., Berger, J. O., George, E. I., and Ročková, V. (2021). The median probability model and correlated variables. *Bayesian Analysis*, 16(4):1085–1112.

- Berk, R. A. (2008). *Statistical Learning from a Regression Perspective*. Springer Nature, Cham, Switzerland, third edition.
- Brilleman, S. L., Elci, E. M., Novik, J. B., and Wolfe, R. (2020). Bayesian survival analysis using the rstanarm R package. *arXiv preprint arXiv:2002.09633*.
- Chouldechova, A. and Hastie, T. (2015). Generalized additive model selection. *arXiv preprint arXiv:1506.03850*.
- Claeskens, G., Krivobokova, T., and Opsomer, J. D. (2009). Asymptotic properties of penalized spline estimators. *Biometrika*, 96(3):529–544.
- Cox, D. R. (1972). Regression models and life-tables. *Journal of the Royal Statistical Society: Series B (Methodological)*, 34(2):187–220.
- de Boor, C. (2001). *A Practical Guide to Splines*. Springer, New York, NY, revised edition.
- Demmler, A. and Reinsch, C. (1975). Oscillation matrices with spline smoothing. *Numerische Mathematik*, 24(5):375–382.
- Eilers, P. H. C. (1999). Comment on “The analysis of designed experiments and longitudinal data by using smoothing splines” by Verbyla, A. P., et al. *Journal of the Royal Statistical Society: Series C (Applied Statistics)*, 48(3):307–308.
- Eilers, P. H. C. and Marx, B. D. (1996). Flexible smoothing with B-splines and penalties. *Statistical Science*, 11(2):89–121.
- Fahrmeir, L., Kneib, T., and Lang, S. (2004). Penalized structured additive regression for space-time data: a Bayesian perspective. *Statistica Sinica*, 14(3):731–761.
- Fahrmeir, L., Kneib, T., Lang, S., and Marx, B. D. (2021). *Regression: Models, Methods and Applications*. Springer, Berlin, second edition.
- Gamerman, D. (1997). Sampling from the posterior distribution in generalized linear mixed models. *Statistics and Computing*, 7(1):57–68.
- George, B., Seals, S., and Aban, I. (2014). Survival analysis and regression models. *Journal of Nuclear Cardiology*, 21(4):686–694.

- George, E. I. and McCulloch, R. E. (1993). Variable selection via Gibbs sampling. *Journal of the American Statistical Association*, 88(423):881–889.
- George, E. I. and McCulloch, R. E. (1997). Approaches for Bayesian variable selection. *Statistica Sinica*, 7(2):339–373.
- Guo, B., Jaeger, B. C., Rahman, A. F., Long, D. L., and Yi, N. (2022). Spike-and-slab least absolute shrinkage and selection operator generalized additive models and scalable algorithms for high-dimensional data analysis. *Statistics in Medicine*, 41(20):3899–3914.
- Hastie, T. and Tibshirani, R. (1986). Generalized additive models. *Statistical Science*, 1(3):297–310.
- Hastie, T. and Tibshirani, R. (1990). *Generalized Additive Models*. Chapman and Hall/CRC Press, Boca Raton, FL.
- He, V. X. and Wand, M. P. (2023). Bayesian generalized additive model selection including a fast variational option. *AStA Advances in Statistical Analysis*.
- Henderson, R., Shimakura, S., and Gorst, D. (2002). Modeling spatial variation in leukemia survival data. *Journal of the American Statistical Association*, 97(460):965–972.
- Hennerfeind, A., Brezger, A., and Fahrmeir, L. (2006). Geoadditive survival models. *Journal of the American Statistical Association*, 101(475):1065–1075.
- Hernández-Lobato, D., Hernández-Lobato, J. M., and Dupont, P. (2013). Generalized spike-and-slab priors for Bayesian group feature selection using expectation propagation. *Journal of Machine Learning Research*, 14(59):1891–1945.
- Hofner, B., Mayr, A., Robinzonov, N., and Schmid, M. (2014). Model-based boosting in R: a hands-on tutorial using the R package mboost. *Computational Statistics*, 29(1-2):3–35.
- Hu, Y., Zhao, K., and Lian, H. (2015). Bayesian quantile regression for partially linear additive models. *Statistics and Computing*, 25(3):651–668.
- Huang, J. Z. (1998). Projection estimation in multiple regression with application to functional ANOVA models. *The Annals of Statistics*, 26(1):242–272.

- Kelker, D. (1970). Distribution theory of spherical distributions and a location-scale parameter generalization. *Sankhyā: The Indian Journal of Statistics, Series A*, 32(4):419–430.
- Klein, N., Carlan, M., Kneib, T., Lang, S., and Wagner, H. (2021). Bayesian effect selection in structured additive distributional regression models. *Bayesian Analysis*, 16(2):545–573.
- Kneib, T. and Fahrmeir, L. (2007). A mixed model approach for geoadditive hazard regression. *Scandinavian Journal of Statistics*, 34(1):207–228.
- Kyung, M., Gill, J., Ghosh, M., and Casella, G. (2010). Penalized regression, standard errors, and Bayesian lassos. *Bayesian Analysis*, 5(2):369–411.
- Lang, S. and Brezger, A. (2004). Bayesian P-splines. *Journal of Computational and Graphical Statistics*, 13(1):183–212.
- Lindgren, F., Rue, H., and Lindström, J. (2011). An explicit link between Gaussian fields and Gaussian Markov random fields: the stochastic partial differential equation approach. *Journal of the Royal Statistical Society: Series B (Statistical Methodology)*, 73(4):423–498.
- Lou, Y., Bien, J., Caruana, R., and Gehrke, J. (2016). Sparse partially linear additive models. *Journal of Computational and Graphical Statistics*, 25(4):1126–1140.
- Martino, S., Akerkar, R., and Rue, H. (2011). Approximate Bayesian inference for survival models. *Scandinavian Journal of Statistics*, 38(3):514–528.
- Mayr, A., Wistuba, T., Speller, J., Gude, F., and Hofner, B. (2023). Linear or smooth? Enhanced model choice in boosting via deselection of base-learners. *Statistical Modelling*, 23(5-6):441–455.
- Neal, R. M. (2003). Slice sampling. *The Annals of Statistics*, 31(3):705–767.
- Nychka, D. and Cummins, D. (1996). Comment on “Flexible smoothing with B-splines and penalties” by Eilers, P. H. C. and Marx, B. D. *Statistical Science*, 11(2):104–105.
- O’Sullivan, F. (1986). A statistical perspective on ill-posed inverse problems. *Statistical Science*, 1(4):502–518.
- Parlett, B. N. (1998). *The Symmetric Eigenvalue Problem*. SIAM, Philadelphia, PA.

- Pérez, M.-E., Pericchi, L. R., and Ramírez, I. C. (2017). The scaled beta2 distribution as a robust prior for scales. *Bayesian Analysis*, 12(3):615–637.
- Ravikumar, P., Lafferty, J., Liu, H., and Wasserman, L. (2009). Sparse additive models. *Journal of the Royal Statistical Society: Series B (Statistical Methodology)*, 71(5):1009–1030.
- Robert, C. P. and Roberts, G. (2021). Rao–Blackwellisation in the Markov chain Monte Carlo era. *International Statistical Review*, 89(2):237–249.
- Ročková, V. (2018). Bayesian estimation of sparse signals with a continuous spike-and-slab prior. *The Annals of Statistics*, 46(1):401–437.
- Rossell, D. and Rubio, F. J. (2023). Additive Bayesian variable selection under censoring and misspecification. *Statistical Science*, 38(1):13–29.
- Ruppert, D. (2002). Selecting the number of knots for penalized splines. *Journal of Computational and Graphical Statistics*, 11(4):735–757.
- Scheipl, F., Fahrmeir, L., and Kneib, T. (2012). Spike-and-slab priors for function selection in structured additive regression models. *Journal of the American Statistical Association*, 107(500):1518–1532.
- Schoenberg, I. J. and Whitney, A. (1953). On Pólya frequency functions. III. The positivity of translation determinants with an application to the interpolation problem by spline curves. *Transactions of the American Mathematical Society*, 74(2):246–259.
- Speckman, P. (1985). Spline smoothing and optimal rates of convergence in nonparametric regression models. *The Annals of Statistics*, 13(3):970–983.
- Stone, C. J. (1986). The dimensionality reduction principle for generalized additive models. *The Annals of Statistics*, 14(2):590–606.
- Stone, C. J. (1994). The use of polynomial splines and their tensor products in multivariate function estimation. *The Annals of Statistics*, 22(1):118–171.
- van de Geer, S. A. (2000). *Empirical Processes in M-estimation*. Cambridge University Press, Cambridge, UK.

- Vershynin, R. (2018). *High-Dimensional Probability: An Introduction with Applications in Data Science*. Cambridge University Press, Cambridge, UK.
- Wahba, G. (1990). *Spline Models for Observational Data*. SIAM, Philadelphia, PA.
- Wand, M. P. and Ormerod, J. T. (2008). On semiparametric regression with O’Sullivan penalized splines. *Australian & New Zealand Journal of Statistics*, 50(2):179–198.
- Wiemann, P., Kneib, T., and Wagner, H. (2021). Effect selection and regularization in structured additive distributional regression. In *Handbook of Bayesian Variable Selection*, pages 271–296. Chapman and Hall/CRC Press, Boca Raton, FL.
- Wood, S. N. (2017). *Generalized Additive Models: An Introduction with R*. Chapman and Hall/CRC Press, Boca Raton, FL, second edition.
- Yuan, M. and Lin, Y. (2006). Model selection and estimation in regression with grouped variables. *Journal of the Royal Statistical Society: Series B (Statistical Methodology)*, 68(1):49–67.
- Zhang, H. H., Cheng, G., and Liu, Y. (2011). Linear or nonlinear? Automatic structure discovery for partially linear models. *Journal of the American Statistical Association*, 106(495):1099–1112.
- Zhou, H. and Hanson, T. (2018). A unified framework for fitting Bayesian semiparametric models to arbitrarily censored survival data, including spatially referenced data. *Journal of the American Statistical Association*, 113(522):571–581.
- Zhou, H., Hanson, T., and Zhang, J. (2020). spBayesSurv: Fitting Bayesian spatial survival models using R. *Journal of Statistical Software*, 92(9):1–33.